ISSN: 0974-2115
www.jchps.com Journal of Chemical and Pharmaceutical Sciences

Finite element analysis of human rib bone and implant design

V Magesh*, S.Sundar
Assistant Professor, Department of Mechanical Engineering, SRM University, Kattankulathur, Kancheepuram, Tamilnadu, India-6030203
*Corresponding author: mageshsrm2004@gmail.com

ABSTRACT

The objective of this Finite Element Analysis (FEA) is to study the force acting on any one of the 24 human rib bones (12 pairs) and to design an implant based on currently available implants with suitable modifications. The superior ribs (numbers 1 to 3) are relatively protected by the scapula, clavicle, and soft tissue, while the inferior "floating" ribs are relatively mobile. Therefore, the more vulnerable middle ribs (numbers 4 to 10) are most susceptible to injury from blunt trauma. For this reason, the left side rib of the 4th pair is taken for this analysis. The model is subjected to an appropriate blunt force, and the deflection is noted. The same blunt force is applied to the ribbed model with the implant, and the deflection is noted. The Ultra-high molecular weight polyethylene (UHMW) and titanium are used as implant materials for the analysis. The results from the above tests are compared and presented in this paper.

Key words: Human rib, Finite element analysis, Blunt force, UHMW, Titanium

1. INTRODUCTION

The thorax is comprised of ribs, thoracic vertebrae, costal cartilage and the sternum. The 12 thoracic vertebrae (T1-T12) and the corresponding ribs form the posterior side of the thorax. Each rib articulates on the vertebrae to facilitate respiration. The anterior surface is formed by the sternum and costal cartilage. The costal cartilage forms a bridge between the central sternum and the first ten ribs. The first seven pairs of ribs connect directly to the sternum through costal cartilage, creating true ribs. The following three pairs join by costal cartilage then attach to the sternum. The two remaining pairs are not attached to the sternum and are termed floating ribs. The curvature of the ribs themselves is greatest for the first rib, and then decreases for the lower ribs. The mechanical aspects of the ribs and their articulations between the sternum and vertebrae are an important part of this study. The articulations between each rib and the sternum create a fixed type of end condition. This fixed end condition allows the production of a bending or torsional moment at the attachment site. This may prove to be an important factor when considering the effects this may have in the way the microstructure of the rib adapts during the life of an individual. The articulations of the ribs with the vertebral column may be classified as more of a pinned condition. This condition allows the rib to rotate slightly, but the translation is limited, therefore, the production of torsional forces in the posterior portion of the rib is limited.

The differences between the articulations of the rib at each end may affect the micro structural adaptation that occurs during life. Hexahedral element and variable thickness shell element for cortical and trabecular bone in the modeling of human ribs suggested that shell element is more efficient and predicted the influence of mesh density, cortical thickness and material properties on human rib fracture and reported that rib models could be done with 2000-3000 coarse mesh solid elements (Zuoping Li, 2010). The studies on various implant system for rib fracture fixation conducted and reported that the combination of anatomic plates and intramedullary splints is the best system to manage the fractures in flail chest injuries (Bottlang, 2010). The age-related shape changes of the human rib cage studies were done and reported that the variation in shape with the age of the human rib cage is significant, and the variation in centroid size with overall body size is also significant (Gayzik, 2008). The intramedullary rib splints for less-invasive stabilization of rib fractures were evaluated and reported that the rib splints provide stability to support respiratory loading throughout the healing phase (Helzel, 2009). Discussion of ribs and intercostal spaces were performed (Ellis, 2008). Studies were conducted on rib fractures with clips and titanium bars and reported that the titanium rib bars and clips provide better clinical results (Santa Barajas, 2010). Studies reported that the injuries take place due to the energy transfer to the body by an impacting object (Viano and King, 2000). The studies showed that chest deflection injury is strongly dependent on age with blunt hub, seat belt, air bag, combined belt and bag (Kent and Patrie, 2005).

FEA of the human rib cage were performed and compared with cadaver test and reported that fracture of 5th rib appears faster and is caused by a smaller force (Awrejccewicz and Luczak, 2007). A case report of first rib fracture reported that the first rib fractures should be considered in the differential diagnosis of patients with upper quadrant pain that is not responsive to conservative care (Nguyen, 2005). The geometry of human ribs studies was done by considering orthopedic chest-wall reconstruction (Mohr, 2007). FEA of human rib fracture under various impact loading conditions were studied (Fang, 2015). FEA on the fatigue fracture of human thoracic cage were performed (Kim, 2015).

Numerous finite-element (FE) models of the human thorax have been developed to understand thoracic structural responses and injuries under various impact loads, including both isolated chest models and whole body models. However, these models utilized only a simplified or generic representation of the actual rib geometry, and

simulated cortical bone by coarse constant-thickness shell elements. Cortical structure varies substantially throughout the rib and thus such simplifications may not be appropriate. Very few FE models of rib segments have been developed and validated against experimental data from individual ribs. Thus the aim of this FEA is to consider left side rib of 4-th pair with blunt force to find deflection. The UHMW and Titanium implants are compared.

2. MATERIALS AND METHODS

Recent advances in computing technologies both regarding hardware and software have helped in the advancement of CAD in applications beyond that of traditional design and analysis. CAD is now being used extensively in the biomedical industry in applications ranging from clinical medicine, customized medical implant design to tissue engineering. The patient-specific computer tomography images of a proximal femur bone are obtained. The 2 mm sliced images are obtained for a height of 68 mm. The 3D voxel model of the bone under study has been made as shown in Fig.1. The image processing is done with the obtained 3D voxel model. The refined model is shown in Fig.2.

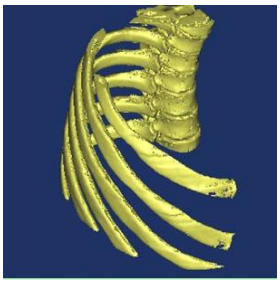

Fig.1.Three-dimensional voxel reconstruction

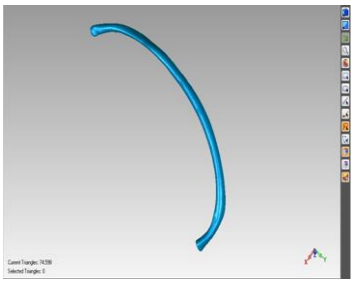

Fig.2.Refined model of the rib

The next face is to generate Non-uniform rational basis spline (NURBS) face of the refine STL model as shown in Fig.3. NURBS is a mathematical model commonly used in computer graphics for generating and representing curves and surfaces which offer great flexibility and precision for handling both analytic (surfaces defined by common mathematical formulae) and modeled shapes. They allow representation of geometrical shapes in a compact form. They can be efficiently handled by the computer programs and yet allow for easy human interaction. NURBS surfaces are functions of two parameters mapping to a surface in three-dimensional space. The implant is modeled using Solid Works software. The implant design specifications are presented in Table 1.

Fig.3.CAD model made from NURBS patches

Table.1.Specifications of implant design

Items	Value(mm)
Length	45 mm
Thickness	2 mm
Diameter for screw(optional)	2 mm

The contour for the design is roughly assumed to that of the rib bone. This is done to facilitate proper fixture during the surgery. For the modeling purposes in a real scenario, Rapid proto-typing techniques can be made use of. Three holes are provided for screws in case the implant tends to be loose during the surgery. But this model is intended to function as a clamp to hold the fractured area in position and thereby to avoid the usage of the screw. But in the case of any discrepancies during the procedure, a screw can be used for securing good clamping. Model of the implant is shown in Fig.4.

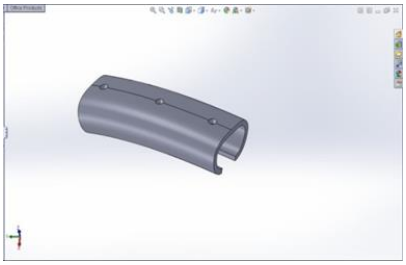

Fig.4.Model of the implant

Bone has non-linear characteristics, and hence its material properties differ in different directions. But for the simplification of the analysis, linear characters were assumed, and suitable material properties were applied based on the literature study. The material properties considered for this study is presented in Table 2. Analysis of the model is done by considering frontal and lateral blunt loading. For blunt frontal loading, three points bending analysis is done. For lateral loading during the crashes which involve side impacts, the role of the seat belts is suppressed and hence we have a single lateral load. During a high-speed crash involving a person of mass 75 kg, the inertial force will be 44.5 kN. So in average, the minimum load on a single rib will be around 3700N.

Table.2.Material properties

Material	Density (kg/m^3)	Young's Modulus (Gpa)	Poisson Ratio
Cortical	2000	11.5	0.3
Trabeculae	1000	0.04	0.45
Titanium	4510	110	0.29
UHMW	970	1.2 to 120	0.46

All tests are performed in the appropriate bending direction to simulate frontal loading of the thorax. The rib specimens removed from the anterior region of the thorax were loaded in the anterior-posterior direction. This placed the interior surface of the rib in tension, which would be expected when the thorax is exposed to seat belt loading during an automobile collision. The lateral rib specimens were loaded in the medial-lateral direction, which placed the exterior surface of these specimens in tension. This loading state at the lateral region of the thorax is due to the compression of the thorax in the anterior-posterior direction during a frontal impact. Finally, the posterior rib specimens were loaded in the posterior-anterior direction, creating tensile forces on the internal surface of the rib specimen.

Finite element analysis: The model is successfully imported to meshing software (Hypermesh), and meshing is done. The inner trabeculae bone was meshed using face extraction of the outer cortical bone. This was done to ensure proper connectivity between the elements of cortical bone and cancellous bone. The elements used for meshing is presented in Table 3. The meshed model of the rib for fracture analysis is shown in Fig.5. The meshed model of the rib-bone implant assembly is shown in Fig.6.

Table.3.Elements used in analysis

Components	Element type	Number of elements
Cortical bone	Solid 45	31432
Cancellous bone	Solid 45	27982
Implant	Solid 185	4692

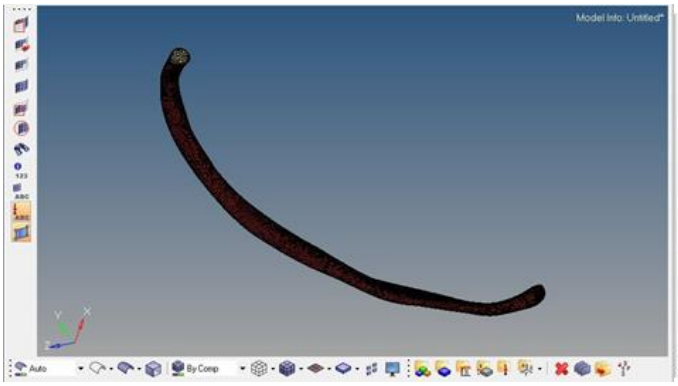

Fig.5. Meshed model of the rib

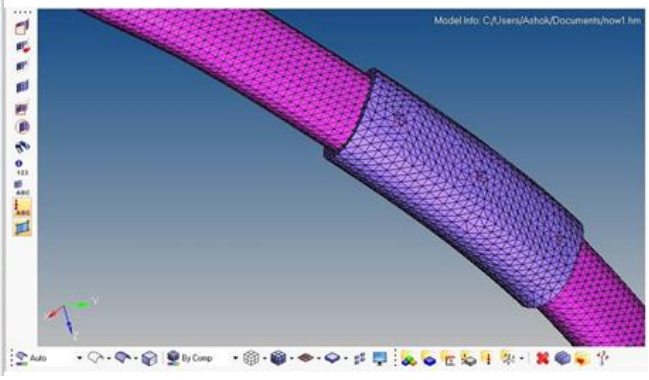

Fig.6. Meshed model of the rib bone- implant

The meshed model is analyzed using Ansys software. During the analysis following assumptions are made: Both the anterior and posterior extremities were assumed to be fixed. Though in reality rib shows a slight movement of about 5mm, they don't come into play during high-speed impacts. So all the Degrees of Freedom were arrested at the extremities. Bone has non-linear characteristics, and hence its material properties differ in different directions. But for the simplification of the analysis, linear characters were assumed, and suitable material properties were applied based on the literature study. Based on the literature surveyed the nominal seat belt loading on the rib was found as 2000N. So this was chosen as the frontal load for the analysis. Fig.7 shows the rib bone for three-point bending. Fig.8 shows the rib with a titanium implant. Fig.9 shows rib with UHMW Polyethylene Implant.

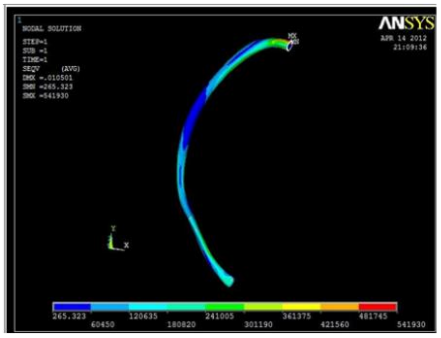

Fig.7. Rib bone under three points bending

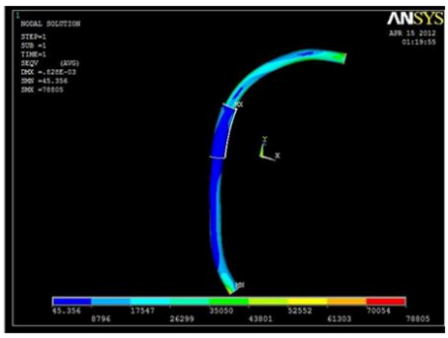

Fig.8. Rib with titanium implant

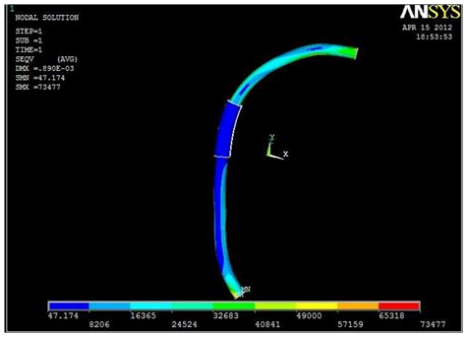

Fig.9. Rib with UHMW implants

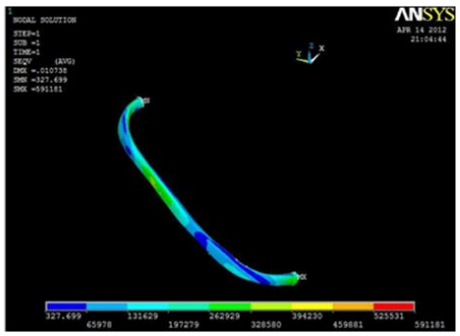

Fig.10 Rib under lateral loading

During the crashes which involve side impacts, the role of the seat belts is suppressed and hence we have a single lateral load. During a high-speed crash involving a person of mass 75 kg, the inertial force will be 44.5 KN. So on average, the minimum load on a single rib will be around 3700N, which is taken as a lateral load. Fig.10 shows the rib under lateral loading. Fig.11 shows Rib with titanium implant under lateral loading. Fig.12 shows Rib with UHMW under lateral loading. All tests were performed in the appropriate bending direction to simulate the frontal loading of the thorax. The rib specimens removed from the anterior region of the thorax were loaded in the anterior-posterior direction. This placed the interior surface of the rib in tension, which would be expected when the thorax is exposed to seat belt loading during an automobile collision. The lateral rib specimens were loaded in the medial-lateral direction, which placed the exterior surface of these specimens in tension. This loading state at the lateral region of the thorax is due to the compression of the thorax in the anterior-posterior direction during a frontal impact. Finally, the posterior rib specimens were loaded in the posterior-anterior direction, creating tensile forces on the internal surface of the rib specimen.

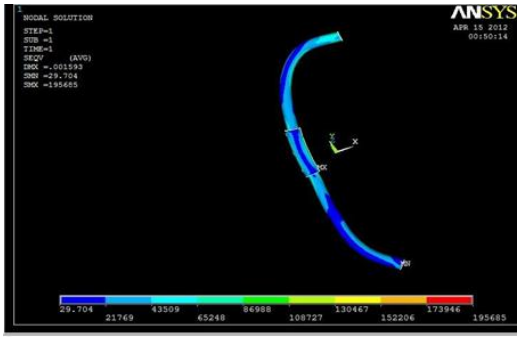

Fig.11.Titanium implant under lateral loading

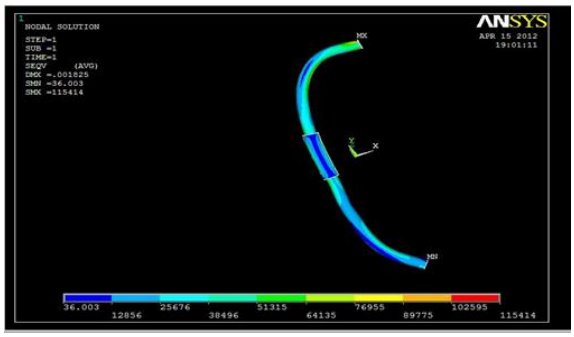

Fig.12.UHMW under lateral loading

3. RESULTS AND DISCUSSION

The finite element analysis of a rib with both implants is successfully done. By considering frontal loading, Fig.7 shows the stress distribution in the rib when subject to three points bending. The red and yellow regions in both extremities show that stress is more concentrated at the ends as they are fixed. In three point bending test, the fracture possibility is more in the region between anterior and lateral portions of the rib. A maximum stress of about 0.54 MPa is developed in the rib. Fig.8 shows the stress distribution in the rib stabilized with a titanium implant. Here a maximum stress is developed on the implant. So the damage to the rib is minimized. Also, the rib deflection is greatly minimized. Fig.9 shows the stress distribution for the same test conducted on the rib with UHMW Polyethylene implant. UHMW has a tensile strength of about 120 GPA. This enables us to create a stronger implant with small

thickness but with more strength. Also, UHMW reinforced with carbon nanotubes has more strength due to the presence of fibers. By considering lateral loading, Fig.10 shows the stress distribution on the rib due to lateral load during side impact on the vehicle.

Table.4.Results of frontal loading

Item	Load (N)	Max. Deflection (mm)
Rib	2000	10.5
Rib with Titanium Implant	2000	0.82
Rib with UHMW Polyethylene Implant	2000	0.89

The stress in this test is concentrated in the lateral region. The deflection is 10.7 mm. The Fig.11 and Fig.12 show the lateral loading stress distribution for the rib with titanium and UHMW implant. The maximum deflection was found as 1.5 mm and 1.8 mm respectively. Table 4 shows the results of frontal loading (three point bend test). Table 5 shows the results of lateral loading.

Table.5.Results of lateral loading

Item	Load(N)	Max. Deflection(mm)
Rib	3700	10.7
Rib with Titanium Implant	3700	1.5
Rib with UHMW Polyethylene	3700	1.8

4. CONCLUSION

The results show that Titanium Implants are better than the UHMW Polyethylene implants, but only by a very small margin. UHMW Polyethylene is suggested over Titanium implants for the following reasons. UHMW polyethylene is much cheaper than the Titanium alloys. Titanium is a rare resource whereas Polyethylene can be synthesized in Laboratories. The inertness of UHMW polyethylene inside the body and its non-toxicity has been already established; UHMW polyethylene does not evoke any immune response just like titanium. Since Polyethylene is flexible, it can adjust during respiration and cause less discomfort for the patients. Also, Polyethylene is better suitable for the clamp like a model to hold the fractured parts intact. It is necessary to take into account the respiratory load for establishing the goodness of the implant. The implant has already been tested with very high lateral loads up to 3700 N. Normal respiratory load on the ribs ranges from 25 N to 50 N in repeated cycles. So this is well below the tested loads, and hence it is established that the implants can endure the respiratory load for a long time without any damage. Future enhancement which can be suggested for this work is to reinforce the UHMW Polyethylene with carbon nanotubes. The main advantage of doing this is that polymer with a tensile modulus of about 120 Gpa can be obtained. The implant can withstand a higher impact force than the currently designed model. Also, further changes in the design can be made to stabilize flail chest injuries. Two implants of the current model joined by a bar can be made. The advantages are: It can be used to support multiple rib fractures. The bar can support the two implants and at the same time moves about the movement of the ribs during respiration.

REFERENCES

Zuoping Li, Matthew Kindig W, Jason R. Kerrigan, Costin DUntaroiu, Damien Submit, Jeff R.Crandall, Richard W. Kent, Rib fractures under anterior–posterior dynamic loads: Experimental and finite-element study, Journal of Biomechanics, 43, 2010, 228- 234.

Bottlang M, Walleser S, Noll M, Honold S, Madey S M, Fitzpatrick D, Long W B, Biomechanical rationale and evaluation of an implant system for rib fracture fixation, European Journal of Trauma and Emergency Surgery, 36, 2010, 417-426.

Francis S. Gayzik, Mao M. Yu, Kerry A. Danelson, Dennis E. Slice, Joel D Stitzel, Quantification of age-related shape change of the human rib cage through geometric morphometrics, Journal of Biomechanics, 41, 2008, 1545-1554.

Inga Helzel, William Long, Daniel Fitzpatrick, Steven Madey, Michael Bottlang, Evaluation of intramedullary rib splints for less-invasive stabilization of rib fractures, Injury international journal of the care of the injured, 40, 2009,1104-1110.

Harold Ellis, The ribs and intercostal spaces, Anaesthesia and Intensive care Medicine, 2008, 518-519.

Pablo Moreno De La Santa Barajas, María Dolores Polo Otero, Carlos Delgado Sánchez-Gracián, Manuel Lozano Gómez, Alberto Toscano Novella, Julia Calatayud Moscoso Del Prado, Sonsoles Leal Ruiloba, Maria L. Choren Duráne, Surgical fixation of rib fractures with clips and titanium bars (STRATOSTM System). Preliminary experience, *Cirugía española*, 88(3), 2010, 180-186.

Viano DC, King AI, Biomechanics of Chest and Abdomen Impact, The Biomedical Engineering Handbook:Second Edition. CRC Press LLC, 2000.

Richard Kent, Jim Patrie, Chest deflection tolerance to blunt anterior loading is sensitive to age but not load distribution, Forensic Science International, 2005, 149, 121–128.

Jan Awrejccewicz, Bartosz Łuczak, The finite element model of the human rib cage, 2007, 45(1), 25-32.

Hang T Nguyen, Joel P Carmichael, J. Scott Bainbridge, Craig Kozak, First tib fracture of unknown etiology: A case report, 29(7), 2005, 590-594.

Marcus Mohr, Eduard Abrams, Christine Engel, William B. Long, Michael Bottlang, Geometry of human ribs pertinent to orthopedic chest-wall reconstruction, Journal of Biomechanics, 40, 2007, 1310-1317.

Wang Fang, Yang Jikuang, Li Guibing, Finite element analysis of human rib under various impact loading conditions, Chinese Journal of Theoretical and Applied Mechanics, 46(2), 2014, 300-307. Antona-Makoshi J, Yamamoto Y, Kato R, sato F, Ejima S, Dokko Y, Yasuki T, Age dependent factors affecting thoracic responses: a finite element study focused on Japanese elderly occupants, Traffic Injury Prevention, 2015, 66-74.

Jung Ho Kim, Sungmin Kim, Honk Seok Lim, Finite element analysis of the fatigue fracture, by age of human throacic cage undergoing dynamic loads, Proceedings of 3rd International Conference on Materials and Reliability Jeju, Korea, 2015, 319-320.